Supporting information for

Vanadium-Doped NiS_2 Porous Nanosphere with High Selectivity and Stability for Electroreduction of Nitrogen to Ammonia

Mingzhu Zhao,[†#] Chengying Guo,[†#] Lingfeng Gao, [*†] Xuan Kuang,[†] Hua Yang, [‡] Xiaojing Ma,[†] Chengqing Liu,[†] Xuejing Liu, [*†] Xu Sun [*†] and Qin Wei[†]

[†]Key Laboratory of Interfacial Reaction & Sensing Analysis in Universities of Shandong, School of Chemistry and Chemical Engineering, University of Jinan, Jinan 250022, Shandong, China.

[‡]Shandong Provincial Key Laboratory of Chemical Energy Storage and Novel Cell Technology, School of Chemistry and Chemical Engineering, Liaocheng University, Liaocheng, 252059, P. R. China.

[#] Mingzhu Zhao and Chengying Guo contributed equally to this work.

Table of contents

1. Material characterizations

The crystal phase of the materials was analysed by an X-ray diffractometer (XRD, Rigaku D/max 2500). The morphologies of the samples were examined by Helios FIB SEM at 10.0 kV. Transmission electron microscopy (TEM, H-800 microscope, Hitachi, Japan) instruments carried with energy dispersive X-ray spectroscopy (EDS). X-ray photoelectron spectroscopy (XPS) was used for analyze the surface chemical composition of the materials.

1.1 Preparation of $Ni(OH)_2$ and vanadium doped $Ni(OH)_2$ (VNOH)

The vanadium doped $Ni(OH)_2$ (VNOH) was prepared successfully via a simple one-step hydrothermal method. Firstly, 1.4 mmol urea (CH_4N_2O) and 0.01 mmol trisodium citrate ($C_6H_5O_7Na_3 \cdot 2H_2O$) were dissolved in 40 mL deionized water (DI) to form the mixed solution. Then, 0.24 mmol ammonium metavanadate (NH_4VO_3) and 0.96 mmol nickel nitrate ($NiNO_3 \cdot 6H_2O$) (with the V/Ni ratio of about 1/4) were added into the solution to form pre-reaction liquid with the magnetic stirring, which was then transferred to 50 mL Teflon-lined stainless steel autoclave, and kept at 150 °C for 24 h. After it was naturally cooling to the room temperature, the as-prepared product was washed and dried under vacuum at 60 ^oC for about 6 h. For better comparison, a series VNOH precursors were synthesized according to the above mentioned method with the V/Ni ratios being 1/2, 1/5, 1/ 6 and 1/8, respectively. Meanwhile, the pure $Ni(OH)_2$ was synthesized as well via the above method, except that no NH_4VO_3 being added.

1.2 Preparation of NiS_2 and pure V-doped NiS_2

The pure NiS_2 and V-doped NiS_2 were synthesized via the high temperature annealing treatment, with thiourea (CH_4N_2S) being adopted as the sulfur source. In detail, 0.8 g CH_4N_2S and 50 mg $Ni(OH)_2$ or VNOH precursor were put at the upstream and downstream in the tube furnace, respectively. The nitrogen gas was adopted as the carrier gas. Then, the samples were annealed at 350 °C for 3 h.

1.3 Preparation of the electrode

The as synthesized NiS_2 or V-NiS_2 catalyst (5 mg) and the 0.5% Nafion solution (5 μL) were dispersed in the 1 mL specially-made solution (V_{water}:$V_{ethanol}$=1:1), which was then ultrasonicated for 1 h to get a well dispersed catalyst ink. Then, 20 μL of the homogeneous ink was loaded onto a carbon paper electrode with an area of 1×1 cm^2 and dried under ambient conditions.

1.4 Electrochemical measurements

The electrocatalytic nitrogen reduction was carried out using a three-electrode system, which include the prepared electrode, carbon rod and Ag/AgCl electrode, respectively. The whole experiments were in the two-compartment cell and separated by the Nafion 211 membrane under the ambient temperature and pressure. The electrochemical tests were carried out in the 0.1 M HCl

solution.

1.5 Determination of NH_3

The indophenol blue method was adopted to quantify the quantity of NH_3 in 0.1 M HCl solution via spectrophotometrically. To produce the calibration curve, for the first step, 1.0 μg mL^{-1} NH_4^+ solution in 0.1 M HCl was prepared used NH_4Cl as raw material, then, it was diluted to a series concentrations (0, 0.1, 0.2, 0.3, 0.4, 0.5, 0.6, 0.6, 0.8, 0.9, 1.0 μg mL^{-1}) using 0.1 M HCl. Take 2 mL reference solution in glass bottle for next color reaction. Next, for the color reaction, 2 mL of 1.0 M NaOH solution (containing 5 wt % salicylic acid and 5 wt % sodium citrate) was added in to 2 mL reference solution in a glass bottle, followed by 1 mL of 0.05 M sodium hypochlorite and 200 μL of 1 wt % sodium nitroferricyanide was also added. After two hours under avoid light, the pure 0.1 M HCl solution was used as calibration. The absorbance at λ=655 nm was collected and plotted (**Figure S8**). The measurement method of the electrolyte of electrolysis for two hours was similar with the above method. The plotting of calibration curve in 0.1 M HCl condition is obtained as well.

1.6 Determination of hydrazine hydrate

The N_2H_4 concentration was recorded by the Watt and Chrisp method. The color developing agent was the mixture of of Para-(dimethylamino) benzaldehyde (5.99 g), HCl (12 M, 30 mL) and ethanol (300 mL). To get the standard curve, a series of 5 mL standard solutions (0, 0.1, 0.2, 0.3, 0.4, 0.5, 0.6, 0.7, 0.8, 0.9, 1.0 μg mL^{-1}) were added with the color reagent (5 mL) and then were placed in the dark environment (20 min). The background correction was carried out using the 0.1 M HCl solution. The absorbance of the reaction liquids was measured at λ=455 nm, and ploted the fitted curve, which showed a good linear relation of the absorbance with the N_2H_4 concentration (y=0.0426+0.710x，**Figure S10**).

1.7 Calculation of NH_3 yield

$$NH_3 \text{ yield} = (c_{NH3} \times V)/t \times m$$

Where c_{NH3} is calculated NH_3 concentration, V is the volume of the electrolyte in the electrolytic tank (50 mL), t is reaction time (2 h), m is the catalyst mass (mg).

1.8 Calculation of Faradaic Efficiency (FE)

According to the standard curve, the concentrations of NH_3 and NH_4^+ were calculated as follows:

$$FE = 3 \times F \times c_{NH3} \times V/Q \times 1000000$$

Where F is the Faradaic constant, Q is the quantity of applied electricity.

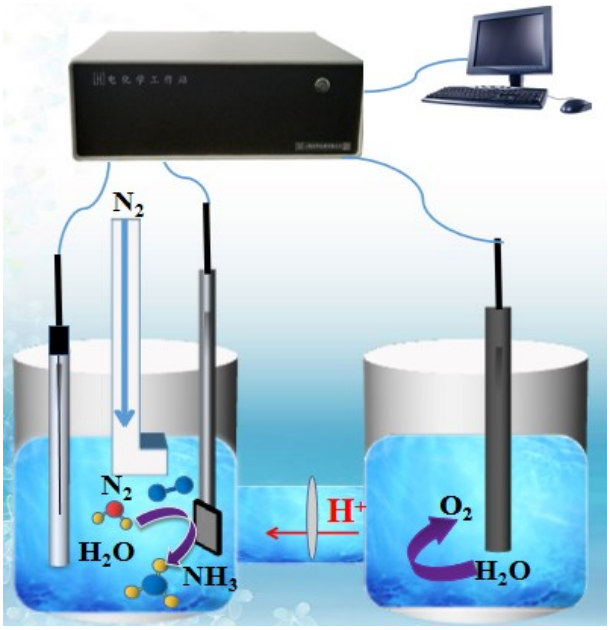

Figure S1. Schematic to illustrate the electrocatalytic setup of V-doped NiS_2 for NRR.

2. XRD spectra of precursor

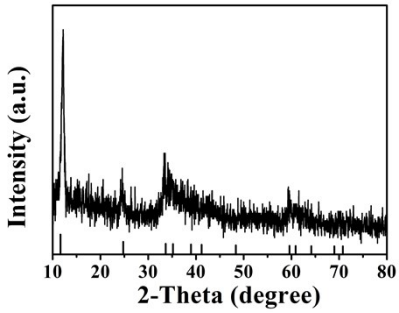

Figure S2. XRD spectra of precursor.

3. XRD spectra of pure NiS_2

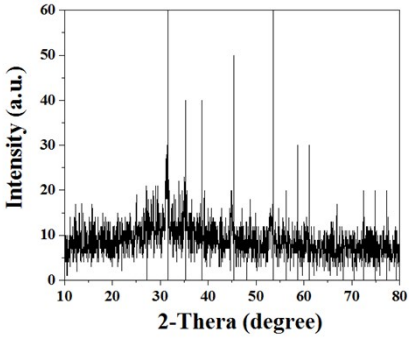

Figure S3. XRD spectra of pure NiS_2

4. XPS survey of $V_{0.2}Ni_{0.8}S_2$

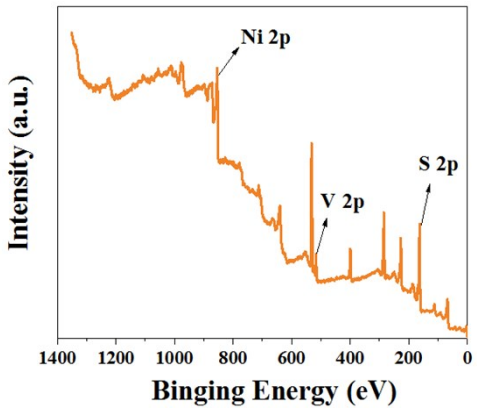

Figure S4. Survey XPS spectral of $V_{0.2}Ni_{0.8}S_2$.

5. SEM image of precursor

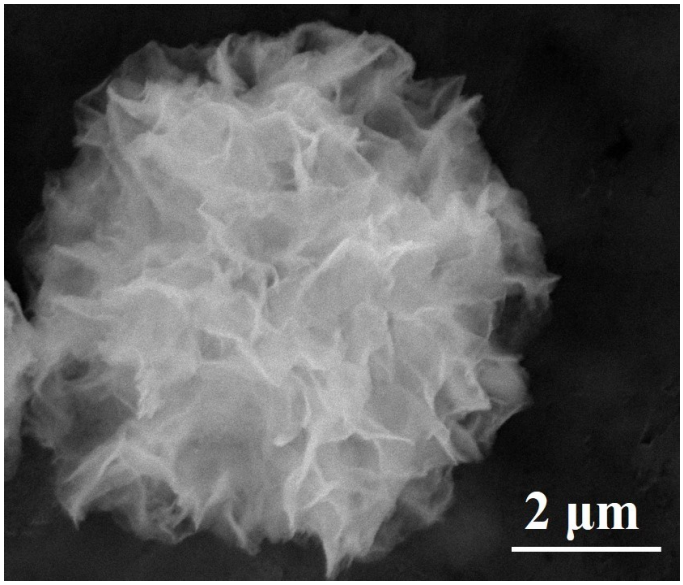

Figure S5. SEM image of precursor.

6. SEM images of pure NiS_2

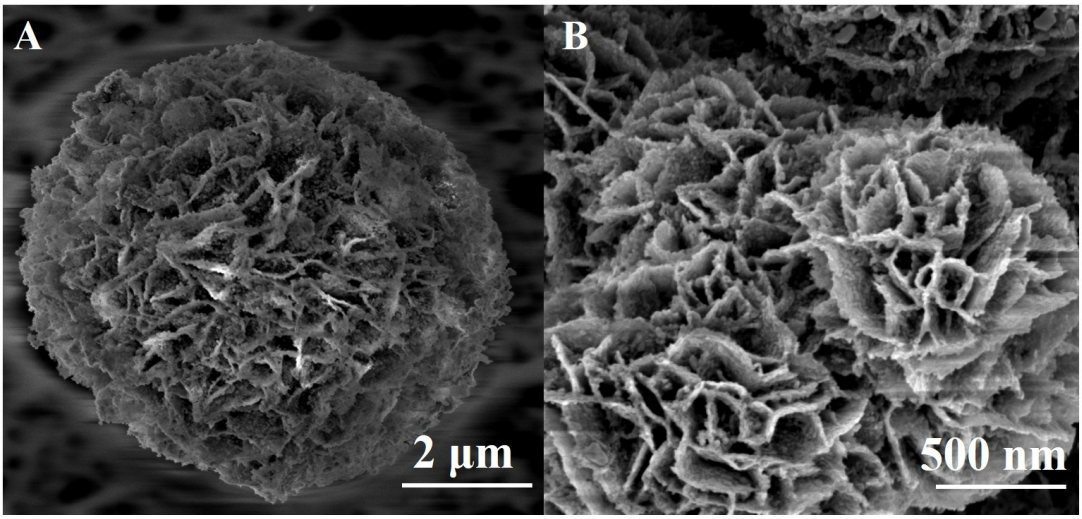

Figure S6. (A) Low- and (B) High-magnification SEM images of pure NiS_2.

7. BET images of pure NiS_2 and $V_{0.2}Ni_{0.8}S_2$

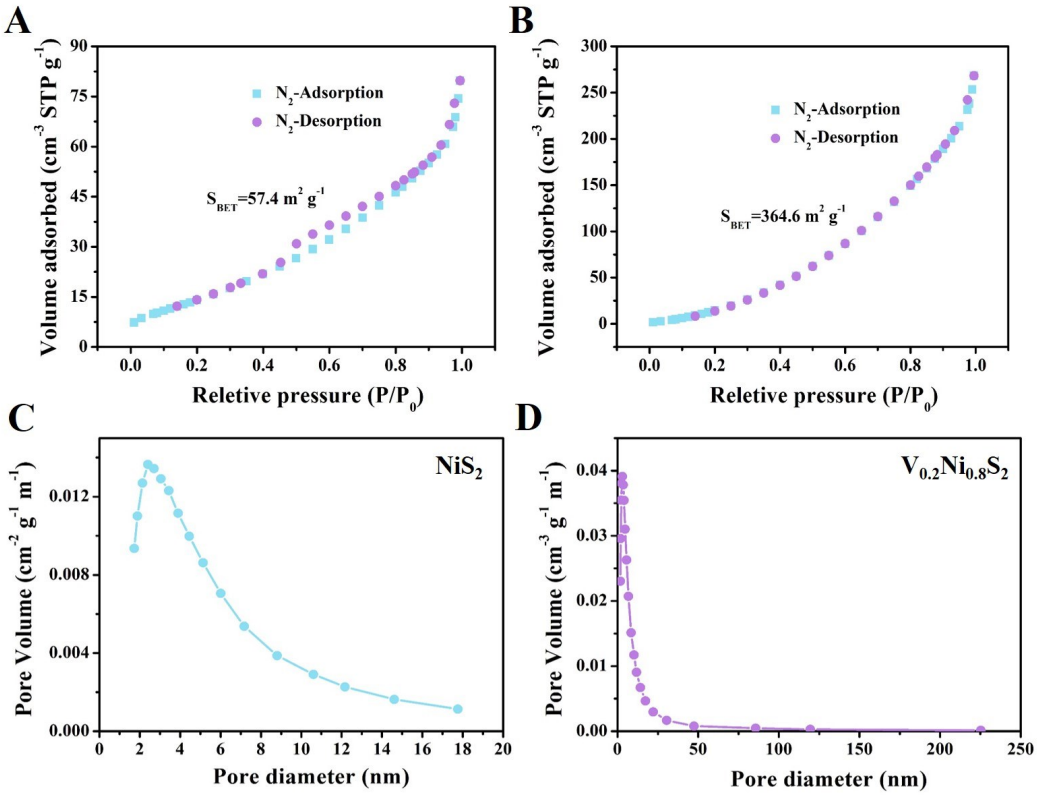

Figure S7. Nitrogen adsorption-desorption isotherms of (A) NiS_2 as well as (B) $V_{0.2}Ni_{0.8}S_2$. Pore size distribution profile of (C) NiS_2 and (D) $V_{0.2}Ni_{0.8}S_2$.

Materials	BET specific surface area / $m^2\ g^{-1}$	BJH average pore diameter / nm	BJT pore volume / $cm^3\ g^{-1}$
$V_{0.2}Ni_{0.8}S_2$	364.6	6.79	0.4159
NiS_2	57.4	4.56	0.1236

Table S1. BET specific surface area and BJH pore volume of $V_{0.2}Ni_{0.8}S_2$ and NiS_2.

8. EDS spectrum of $V_{0.2}Ni_{0.8}S_2$

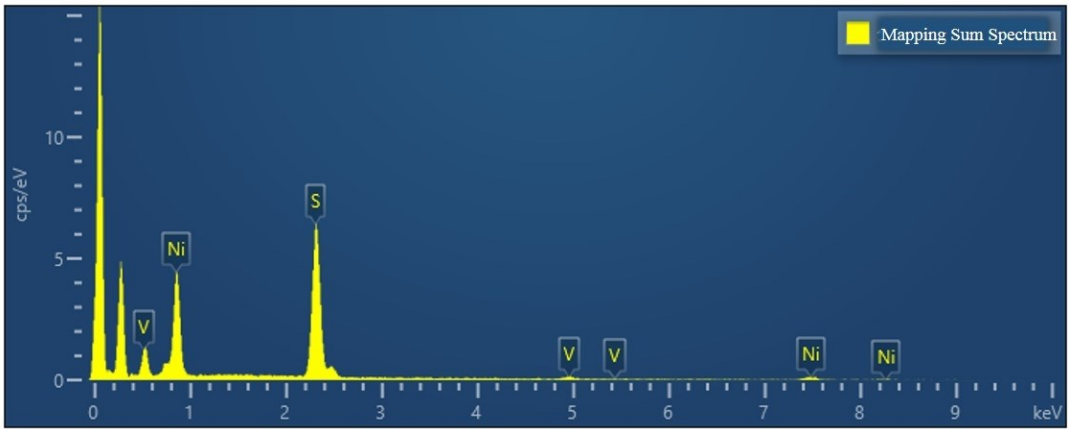

Figure S8. EDS spectrum of $V_{0.2}Ni_{0.8}S_2$.

9. Gas-tight-two-compartment cell for NRR

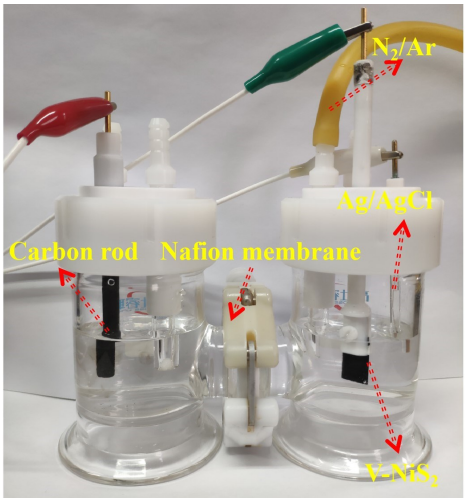

Figure S9. Gas-tight-two-compartment cell for NRR.

10. Standard curve of NH_3

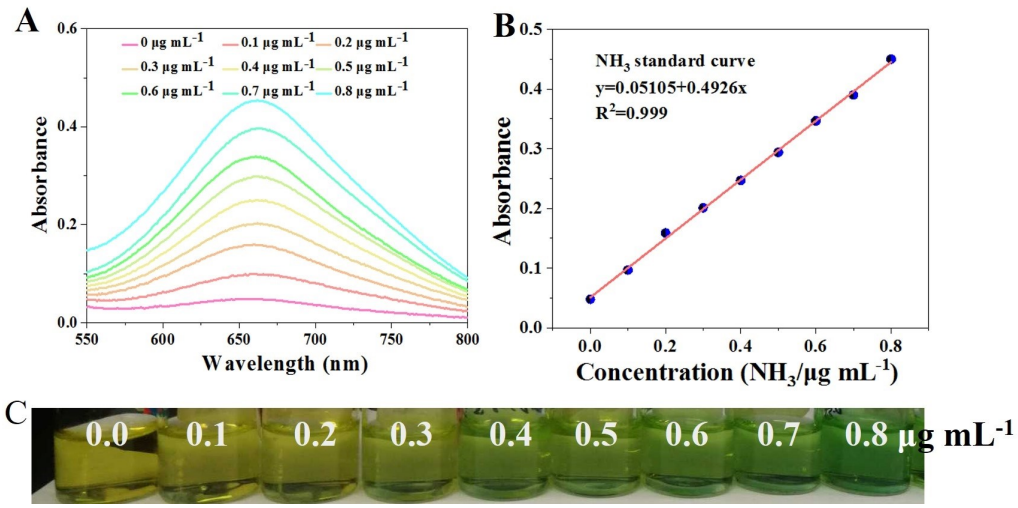

Figure S10. (A) UV-vis absorption spectrums of standard solutions with different NH_4^+ concentration. (B) Standard curve from the NH_4^+ concentration. (C) The chromogenic reaction of indophenol indicator with NH_4^+ of different concentration.

11. UV-vis absorption spectrums of all contrast experiments

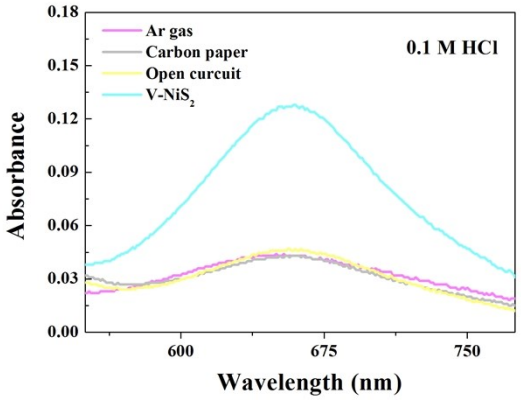

Figure S11. UV-vis absorption spectrums of all contrast experiments including Ar as feed gas, clear carbon paper as working electrode and open circuit.

12. Standard curve of N_2H_4

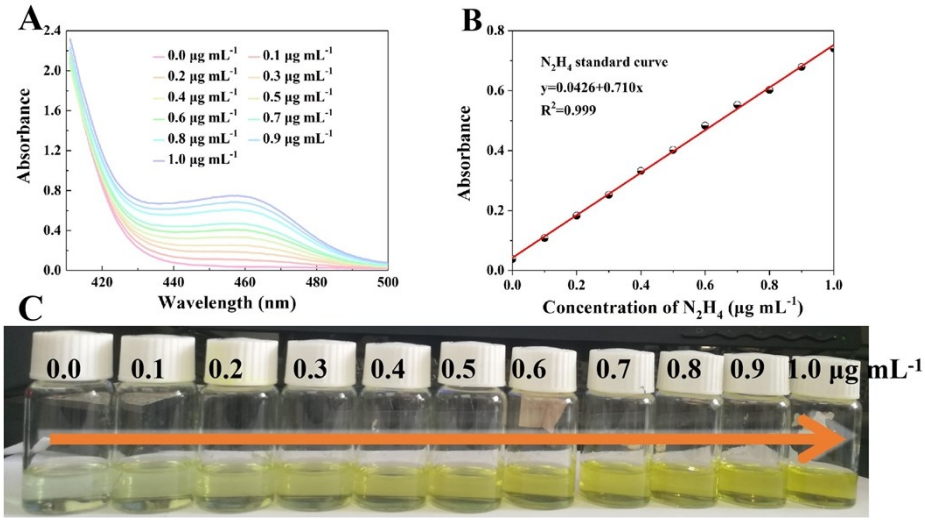

Figure S12. (A) UV-vis curves of a serious of N_2H_4 concentrations after 20 min. (b) Standard curve for the estimation of the concentration of N_2H_4. (C) The chromogenic reaction with corresponding N_2H_4 concentrations.

13. UV-vis spectrum and corresponding N_2H_4 yield

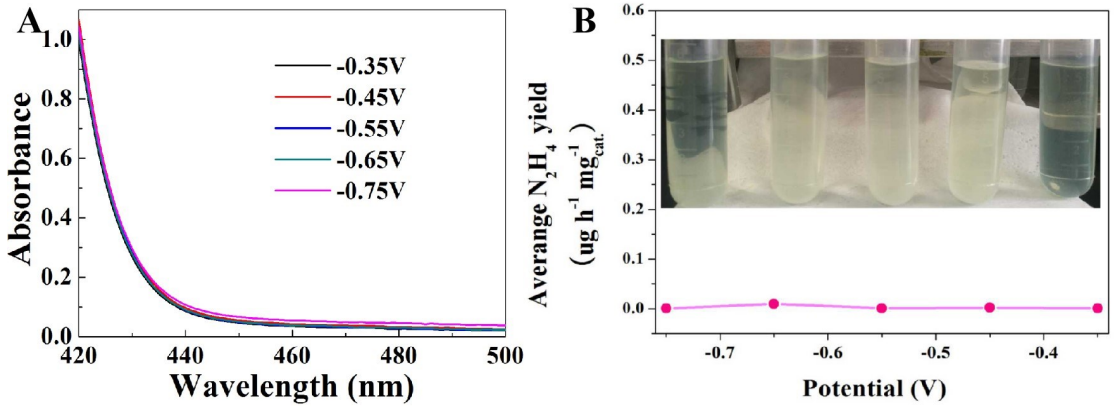

Figure S13. (A) UV-vis curves of $V_{0.2}Ni_{0.8}S_2$ at every potential to detect by-product. (B) Corresponding yield at all potentials, inset: the chromogenic reaction of every potential.

14. Electrocatalytic activity comparison

Material	NH_3 yield/μg h^{-1} $mg^{-1}_{cat.}$	FE
NiS_2	5.8	0.5 %
$V_{0.34}Ni_{0.66}S_2$	21.583	2.9 %

$V_{0.17}Ni_{0.83}S_2$	38.259	6.7 %
$V_{0.14}Ni_{0.86}S_2$	29.921	4.2 %
$V_{0.11}Ni_{0.89}S_2$	24.795	3.5 %

Table S2. Summary of all catalysts for NRR at 0.1 M HCl solution.

15. Comparison with other reported NRR catalysts

Material	Electrolyte	NH_3 yield/μg h^{-1} $mg^{-1}_{cat.}$	FE	Potential/V
This work	0.1 M HCl	47.64	9.70 %	-------
Mo_2N nanorod[1]	0.1 M HCl	78.4	4.50 %	-0.3
Defect-Rich MoS_2Nanoflower[2]	0.1 M Na_2SO_4	29.28	8.34 %	-0.4
Fe-Ni_2P nanosheets[3]	0.1 M HCl	88.51	7.92 %	-0.3
Fe_2O_3 nanorod[4]	0.1 M Na_2SO_4	6.78	7.69 %	-0.4
Mn_3O_4 nanocube[5]	0.1 M Na_2SO_4	11.6	3.0 %	-0.8
Sn/SnS_2 nanosheets[6]	0.1 M NaOH	23.8	6.5 %	-------
Nb_2O_5 nanofiber[7]	0.1 M HCl	43.6	9.26 %	-0.55
Co_3O_4@NCs[8]	0.05 M H_2SO_4	42.58	8.5 %	-0.2
P-CNTs[9]	0.25 M $LiClO_4$	24.4	12.5 %	-------
CaCoOx[10]	0.5 M Na_2SO_4	16.25	20.51	-0.3
CoS nano-flowers[11]	0.05 M H_2SO_4	16.5	12.1	-0.15
Two-dimensional vanadium carbide[12]	0.1 M HCl	23.2	18.3	-0.1
CrN nanocube[13]	0.1 M HCl	31.11	16.6	-0.5
Boron, nitrogen and fluorine ternary-doped carbon[14]	0.05 M H_2SO_4	41	14	-0.4

Table S3. Comparison between $V_{0.2}Ni_{0.8}S_2$ with some other reported NRR catalysts.

References

1. X. Ren, G. Cui, L. Chen, F. Xie, Q. Wei, Z. Tian and X. Sun, Electrochemical N_2 fixation to NH_3 under ambient conditions: Mo_2N nanorod as a highly efficient and selective catalyst. *Chem Commun (Camb)*, 2018, **54**, 8474-8477.
2. X. Li, T. Li, Y. Ma, Q. Wei, W. Qiu, H. Guo, X. Shi, P. Zhang, A. M. Asiri, L. Chen, B. Tang and X. Sun, Boosted Electrocatalytic N_2 Reduction to NH_3 by Defect-Rich MoS_2 Nanoflower， *Adv. Energy Mater.*, 2018, **8**.
3. C. Guo, X. Liu, L. Gao, X. Kuang, X. Ren, X. Ma, M. Zhao, H. Yang, X. Sun and Q. Wei, Fe-doped Ni_2P nanosheets with porous structure for electroreduction of nitrogen to ammonia under ambient conditions, *Appl. Catal. B-Environ.*, 2020, **263**.
4. Z. Wang, K. Zheng, S. Liu, Z. Dai, Y. Xu, X. Li, H. Wang and L. Wang, Interconnected

porous composites electrode materials of Carbon@Vanadium nitride by directly absorbing VO_3, *ACS Sustain. Chem. Eng.*, 2019, **7**, 11754-11759.

5. X. Wu, L. Xia, Y. Wang, W. Lu, Q. Liu, X. Shi and X. Sun, Mn_3O_4 Nanocube: An Efficient Electrocatalyst Toward Artificial N_2 Fixation to NH_3, *Small*, 2018, **14**, e1803111.
6. P. Li, W. Fu, P. Zhuang, Y. Cao, C. Tang, A. B. Watson, P. Dong, J. Shen and M. Ye, Amorphous Sn/Crystalline SnS_2 Nanosheets via In Situ Electrochemical Reduction Methodology for Highly Efficient Ambient N_2 Fixation, *Small*, 2019, **15**, e1902535.
7. J. Han, Z. Liu, Y. Ma, G. Cui, F. Xie, F. Wang, Y. Wu, S. Gao, Y. Xu and X. Sun, Ambient N_2 fixation to NH_3 at ambient conditions: Using Nb_2O_5 nanofiber as a high-performance electrocatalyst, *Nano Energy*, 2018, **52**, 264-270.
8. S. Luo, X. Li, B. Zhang, Z. Luo and M. Luo, *ACS Appl Mater Interfaces*, MOF-Derived Co_3O_4@NC with Core–Shell Structures for N_2 Electrochemical Reduction under Ambient Conditions, 2019, **11**, 26891-26897.
9. L. Yuan, Z. Wu, W. Jiang, T. Tang, S. Niu and J. Hu, Phosphorus-doping Activates Carbon Nanotubes for Efficient Electroreduction of Nitrogen to Ammonia, *Nano Res.*, 2020, 13, 1376–13810.
10. X. Chen, K. Li, X. Yang, J. Lv, S. Sun, S. Li, D. Cheng, B. Li, Y. Li and H. Zang, Oxygen Vacancy Engineering of Calcium Cobaltate: A Nitrogen Fixation Electrocatalyst at Ambient Condition in Neutral Electrolyte, *Nano Res.* 2021, 14, 501–506.
11. C. Li, R Xu, S Ma, Y Xie, K. Qu, H. Bao, W. Cai, Z. Yang, Sulfur vacancies in ultrathin cobalt sulfide nanoflowers enable boosted electrocatalytic activity of nitrogen reduction reaction, *Chen. Eng. J.,* 2020, 415, 129018.
12. C. Zhang, D. Wang, Y. Wan, R. Lv, S. Li, B. Li,X. Zou, S. Yang, Vanadium carbide with periodic anionicvacancies for effective electrocatalyticnitrogen reduction, *Mater. Today*, 2020, 40, 15-18.
13. Z. Ma, J. Chen, D. Luo, Thomas T., Richard D. and Adam S. Structural evolution of CrN nanocubeelectrocatalysts during nitrogen reductionreaction, *Nanoscale*, 2020, 12, 19276–19283.
14. Q. Zhang, F. Luo, Y. Ling, S. Xiao, M. Li, K. Qu, Y. Wang, Ji. Xu, W. Cai and Z. Yang. Identification of functionality of heteroatoms inboron, nitrogen and fluorine ternary-doped carbonas a robust electrocatalyst for nitrogen reductionreaction powered by rechargeable zinc–airbatteries, *J. Mater. Chem. A*, 2020, 8, 8430–8439.